Received: 12 December 2022 | Revised: 31 March 2023 | Accepted: 13 April 2023

DOI: 10.1002/psp4.12981

ARTICLE

Physiologically-based pharmacokinetic modeling of quinidine to establish a CYP3A4, P-gp, and CYP2D6 drug–drug–gene interaction network

Denise Feick[1] | Simeon Rüdesheim[1,2] | Fatima Zahra Marok[1] | Dominik Selzer[1] | Helena Leonie Hanae Loer[1] | Donato Teutonico[3] | Sebastian Frechen[4] | Maaike van der Lee[5] | Dirk Jan A. R. Moes[5] | Jesse J. Swen[5] | Matthias Schwab[2,6,7] | Thorsten Lehr[1]

[1]Clinical Pharmacy, Saarland University, Saarbrücken, Germany

[2]Dr. Margarete Fischer-Bosch-Institute of Clinical Pharmacology, Stuttgart, Germany

[3]Translational Medicine & Early Development, Sanofi-Aventis R&D, Chilly-Mazarin, France

[4]Bayer AG, Pharmaceuticals, Research & Development, Systems Pharmacology & Medicine, Leverkusen, Germany

[5]Department of Clinical Pharmacy & Toxicology, Leiden University Medical Center, Leiden, The Netherlands

[6]Departments of Clinical Pharmacology, Pharmacy and Biochemistry, University of Tübingen, Tübingen, Germany

[7]Cluster of Excellence iFIT (EXC2180) "Image-guided and Functionally Instructed Tumor Therapies", University of Tübingen, Tübingen, Germany

Correspondence
Thorsten Lehr, Clinical Pharmacy, Saarland University, Campus C5 3, 66123 Saarbrücken, Germany.
Email: thorsten.lehr@mx.uni-saarland.de

Abstract

The antiarrhythmic agent quinidine is a potent inhibitor of cytochrome P450 (CYP) 2D6 and P-glycoprotein (P-gp) and is therefore recommended for use in clinical drug–drug interaction (DDI) studies. However, as quinidine is also a substrate of CYP3A4 and P-gp, it is susceptible to DDIs involving these proteins. Physiologically-based pharmacokinetic (PBPK) modeling can help to mechanistically assess the absorption, distribution, metabolism, and excretion processes of a drug and has proven its usefulness in predicting even complex interaction scenarios. The objectives of the presented work were to develop a PBPK model of quinidine and to integrate the model into a comprehensive drug–drug(–gene) interaction (DD(G)I) network with a diverse set of CYP3A4 and P-gp perpetrators as well as CYP2D6 and P-gp victims. The quinidine parent-metabolite model including 3-hydroxyquinidine was developed using pharmacokinetic profiles from clinical studies after intravenous and oral administration covering a broad dosing range (0.1–600 mg). The model covers efflux transport via P-gp and metabolic transformation to either 3-hydroxyquinidine or unspecified metabolites via CYP3A4. The 3-hydroxyquinidine model includes further metabolism by CYP3A4 as well as an unspecific hepatic clearance. Model performance was assessed graphically and quantitatively with greater than 90% of predicted pharmacokinetic parameters within two-fold of corresponding observed values. The model was successfully used to simulate various DD(G)I scenarios with greater than 90% of predicted DD(G)I pharmacokinetic parameter ratios within two-fold prediction success limits. The presented network will be provided to the research community and can be extended to include further perpetrators, victims, and targets, to support investigations of DD(G)Is.

This is an open access article under the terms of the Creative Commons Attribution-NonCommercial License, which permits use, distribution and reproduction in any medium, provided the original work is properly cited and is not used for commercial purposes.
© 2023 The Authors. *CPT: Pharmacometrics & Systems Pharmacology* published by Wiley Periodicals LLC on behalf of American Society for Clinical Pharmacology and Therapeutics.

Study Highlights

WHAT IS THE CURRENT KNOWLEDGE ON THE TOPIC?

Quinidine is an inhibitor of cytochrome P450 (CYP) 2D6 and P-gp as well as a substrate of CYP3A4 and P-gp. It is recommended for use in clinical drug–drug interaction studies.

WHAT QUESTION DID THIS STUDY ADDRESS?

Quinidine pharmacokinetics were extensively studied applying physiologically-based pharmacokinetic (PBPK) modeling. Furthermore, its interaction potential was assessed within a comprehensive CYP2D6-CYP3A4-P-gp drug–drug–gene interaction (DDGI) network, involving quinidine as both perpetrator and victim drug.

WHAT DOES THIS STUDY ADD TO OUR KNOWLEDGE?

The in vivo interaction potential of quinidine could be accurately modeled, emphasizing the potential of the PBPK approach to investigate even complex DDGI scenarios.

HOW MIGHT THIS CHANGE DRUG DISCOVERY, DEVELOPMENT AND/OR THERAPEUTICS?

This work highlights the evaluation of PBPK models in the context of a complex interaction network. The quinidine model can assist in future investigations on CYP2D6-CYP3A4-P-gp DDGIs during model-informed drug development.

INTRODUCTION

Cytochrome P450 (CYP) 2D6 is thought to be involved in the metabolism of about 20–25% of drugs and exhibits a highly polymorphic expression.[1] Consequently, CYP2D6 drug–gene interactions (DGIs) adversely affecting drug pharmacology frequently occur in clinical practice. Additionally, the concomitant administration of drugs can also modulate CYP2D6 metabolism, potentially resulting in drug–drug–gene interactions (DDGIs) which may further increase the risk of adverse drug reactions (ADRs).[2] Here, drug-induced CYP2D6 phenoconversion (i.e., the conversion from normal to poor metabolizer phenotypes due to the co-administration of strong inhibitors), has been described in the literature with varying magnitudes of interaction effects in different CYP2D6 phenotypes.[3]

Quinidine is a class 1A anti-arrhythmic drug and acts by blocking voltage-gated sodium channels. Due to its high risk for side effects and interaction potential as well as the availability of more advantageous anti-arrhythmic treatment options, the clinical relevance of quinidine has been in decline with steadily decreasing prescription rates over the last decades.[4] However, as a strong CYP2D6 inhibitor and inhibitor of P-glycoprotein (P-gp), quinidine is still used in clinical drug–drug interaction (DDI) studies, as recommended by the US Food and Drug Administration (FDA).[5] Here, the investigation of these interactions can provide valuable insights into the involved absorption, distribution, metabolism, and excretion (ADME) processes of concomitantly administered CYP2D6 and P-gp substrates.

Quinidine exhibits extensive hepatic and intestinal first-pass metabolism.[6] For this, CYP3A4 was found to be the most important enzyme in vitro and researchers have proposed to utilize quinidine 3-hydroxylation as a specific in vitro marker reaction for CYP3A4 activity.[7] Furthermore, quinidine has been identified as a substrate of P-gp in vitro,[5] making it susceptible to DDIs involving CYP3A4 and P-gp. Quinidine displays nonlinear pharmacokinetics that can be attributed to a saturation of intestinal CYP3A4 and P-gp.[8] Although quinidine shares structural similarities with many CYP2D6 substrates, the contribution of CYP2D6 to the metabolism of quinidine is negligible.[7] However, due to its high affinity to the metabolic site of CYP2D6, quinidine is a potent competitive inhibitor of CYP2D6.[9] Its metabolites have been found to contribute to the inhibition of CYP2D6.[10]

Several DDGI studies have been published investigating the effect of CYP2D6 polymorphisms and quinidine administration on victim drug pharmacokinetics (e.g., metoprolol[11]), resulting in considerable increases in drug exposure. Here, innovative tools are required to investigate DDGIs, as performing dedicated clinical trials routinely in drug development is infeasible due to combinatorical complexities and can put study subjects at a considerable risk of experiencing ADRs.[2] For this, physiologically-based pharmacokinetic (PBPK) modeling is a powerful

mechanistic approach to model the pharmacokinetics of a drug, taking an individual's physiological and genetic profile into account.[2] Thoroughly built and evaluated PBPK models can be valuable to describe the underlying ADME processes and investigate even complex DD(G)I scenarios.[2] Furthermore, these models can assist in generating and testing hypotheses regarding, for instance, (patho-) physiological changes affecting ADME processes where in vitro and in vivo data are incomplete or inconclusive.[12] Mechanistic DGI models have shown their usefulness in describing and predicting the effect of polymorphisms on drug pharmacokinetics (e.g., for the CYP2D6 substrates metoprolol and dextromethorphan), demonstrating how PBPK models can assist in understanding the underlying ADME-related processes and explain observed interindividual variability.[13,14] PBPK DD(G)I networks can have enormous potential in this area, as evaluated models can support simulating untested DD(G)I scenarios and support model-informed drug discovery and development.[15]

Due to the importance of quinidine as DDI probe drug for CYP2D6 and P-gp inhibition as well as CYP3A4 and P-gp substrate, the main objectives of this work were (i) to develop a comprehensive PBPK model of quinidine and its major metabolite 3-hydroxyquinidine and (ii) to predict complex quinidine DD(G)Is within a comprehensive PBPK interaction network involving CYP3A4, CYP2D6, and P-gp.

METHODS

Software

The development of the quinidine PBPK model, parameter optimizations, and sensitivity analysis, as well as simulation of different DD(G)I scenarios were performed with PK-Sim (version 11, Open Systems Pharmacology Suite, www.open-systems-pharmacology.org). Published plasma concentration-time profiles were digitized with Engauge Digitizer 10.12 (M. Mitchell, https://markummitchell.github.io/engauge-digitizer). Model evaluations (i.e., graph generation and calculation of pharmacokinetic parameters as well as statistics) were accomplished using the R programming language version 4.2.1 (The R Foundation for Statistical Computing, Vienna, Austria) and Rstudio 2022.07.0 (Rstudio).

Quinidine PBPK model building

PBPK model building was initialized by collecting physicochemical and ADME-related parameters of quinidine and 3-hydroxyquinidine from the literature. Additionally, studies reporting quinidine and 3-hydroxyquinidine plasma concentrations alongside subject information and administration protocols were collected. Studies were preferably included if performed in healthy volunteers and if concentration-time profiles were reported alongside unambiguous dosing and regimen information. Gathered concentration-time profiles were split into a model training (model development) and a test dataset (model evaluation). The model training dataset was assembled to (i) maximize the cardinality of the test dataset and to cover (ii) intravenous and oral administration, (iii) the whole dosing range of published studies, and (iv) single and multiple dose administration while preferring information-dense as well as (v) additional measurements of 3-hydroxyquinidine profiles. Virtual individuals ("mean individuals") were created based on the mean and mode of the reported study demographics if available. By selecting ethnicities according to the study cohorts from the PK-Sim database, varying organ volumes and perfusion rates were taken into account. Relevant enzymes and transporters were implemented according to literature reports and the PK-Sim expression database (see Tables S1–S3). Parameter optimizations were performed to identify suitable quantitative structure–activity relationship methods to calculate cellular permeabilities and partition coefficients. Furthermore, model parameter values that could not be informed from literature reports (e.g., quinidine intestinal permeability as well as relevant catalytic and transport rate constants) were optimized by fitting model simulations against all studies of the training dataset applying Monte Carlo optimization minimizing the least-squares objective function.[16]

Quinidine PBPK model evaluation

Model performance was evaluated graphically by comparison of population simulation predictions and observed quinidine and 3-hydroxyquinidine plasma concentration-time profiles. For this, virtual populations of 1000 individuals were generated, based on the study demographics listed in the respective publications, such as ethnic background as well as age and weight range. Additional variability regarding the expression of metabolizing enzymes and transporters was implemented according to the PK-Sim ontogeny database (see Table S1).

Furthermore, predicted plasma concentrations for mean individuals, area under the plasma concentration-time curve calculated between the first and last concentration measurement (AUC_{last}) and maximum plasma concentration (C_{max}) values were compared to their respective observed values in goodness-of-fit plots by

assessing the proportion of predictions within two-fold of observed concentration, AUC_{last} and C_{max} data. As quantitative measures to evaluate the model performance, mean relative deviations (MRDs) for all predicted concentration-time profiles and geometric mean fold errors (GMFEs) for all predicted AUC_{last}, C_{max}, apparent volume of distribution (V_d) and half-life values were calculated as previously described.[13,17] Predictions with MRDs and GMFEs less than two were considered successful.

To assess the influence of single parameter changes on model-simulated AUC, a local sensitivity analysis was performed using a parameter perturbation of 1000%. Parameters were considered sensitive if their sensitivity value was equal or greater than 0.5. More details on the conducted local sensitivity analysis are provided in Supplement S1 (Section S2.10).

DD(G)I modeling network building

To assess the performance of the newly developed quinidine model to predict various DD(G)I scenarios, the model was linked to previously published PBPK models of carbamazepine,[18] cimetidine,[12] fluvoxamine,[19] itraconazole,[20] R-/S-omeprazole,[21] rifampicin,[20] and R-/S-verapamil[22] (here, quinidine is acting as CYP3A4 and P-gp victim drug) as well as to models of dextromethorphan,[14] digoxin,[20] metoprolol,[13] mexiletine,[21] and paroxetine[23] (here, quinidine is acting as an inhibitor of CYP2D6 and P-gp). Moreover, CYP2D6 DDGI scenarios with dextromethorphan, metoprolol, and mexiletine were modeled by adjusting CYP2D6 activity related to the phenotype (normal and poor metabolizers) according to previous modeling work.[13,14,21] For all simulated interactions, the quinidine inhibitory constant (K_i) values were kept constant over the whole range of CYP2D6 activity.

DD(G)I modeling network evaluation

DD(G)I model performances were evaluated by comparing victim drug population predictions with observed plasma concentrations alone and during perpetrator co-administration. Furthermore, predicted compared to observed DD(G)I pharmacokinetic parameter ratios (ratios between AUC_{last} or C_{max} during the DD(G)I and of the victim drug alone) were plotted in goodness-of-fit plots. Here, limits for the assessment of DD(G)I ratios were applied according to Guest et al.[24] including 20% variability. Additionally, GMFEs of DD(G)I AUC_{last} and C_{max} ratios were calculated.

RESULTS

Quinidine PBPK model

A comprehensive quinidine-3-hydroxyquinidine parent-metabolite whole-body PBPK model was built and evaluated using data from 22 clinical studies reporting a total of 43 plasma concentration-time profiles for quinidine. Additionally, two profiles of unbound quinidine and eight plasma concentration-time profiles of 3-hydroxyquinidine were included in the model datasets. In these studies, plasma concentration-time profiles were reported after single intravenous administration of 260.3–520.6 mg quinidine gluconate (corresponding to 162.2–324.4 mg quinidine base) and single or multiple oral administrations of 0.1–600 mg quinidine sulfate (corresponding to 0.08–497.2 mg quinidine base). The training dataset included 10 profiles of quinidine in plasma, two profiles of quinidine in urine, and five profiles of 3-hydroxyquinidine in plasma. Information about all utilized studies, including the demographics and implemented ethnicities of study subjects, is provided in Tables S4, S13, and S14. Efflux transport of quinidine via P-gp was incorporated and metabolism via CYP3A4 (saturable Michaelis–Menten kinetics) was implemented for the building of 3-hydroxyquinidine and other unspecific metabolites. The 3-hydroxyquinidine metabolism was modeled via CYP3A4 and an unspecific hepatic clearance process as a surrogate for further unspecified enzymes (both first-order kinetics). Renal excretion of both compounds was modeled as passive glomerular filtration. Additionally, active tubular secretion via P-gp transport was incorporated in the model for quinidine. For oral formulations (quinidine sulfate immediate release), a Weibull dissolution was incorporated. All relevant quinidine and 3-hydroxyquinidine drug-dependent parameters are listed in Table S5, information about the expression and localization of relevant proteins is provided in Tables S1–S3.

A selection of population predictions of quinidine and 3-hydroxyquinidine compared to their respective observed data after intravenous and oral administration is shown in Figure 1a–f. Semilogarithmic and linear plots of all modeled studies are shown in Figures S1–S14. The good descriptive and predictive model performance is displayed in goodness-of-fit plots (Figures 1g–i, S15, S16), where 94%, 100%, and 100% of quinidine training dataset, 90%, 97%, and 91% of quinidine test dataset, 79%, 100%, and 80% of 3-hydroxyquinidine training dataset and 89%, 100%, and 100% of 3-hydroxyquinidine test dataset predicted plasma concentrations, AUC_{last} and C_{max} values were within two-fold of the corresponding observed values, respectively. Moreover, nine of 10 quinidine training dataset, 30 of 33 quinidine test dataset, five of five 3-hydroxyquinidine

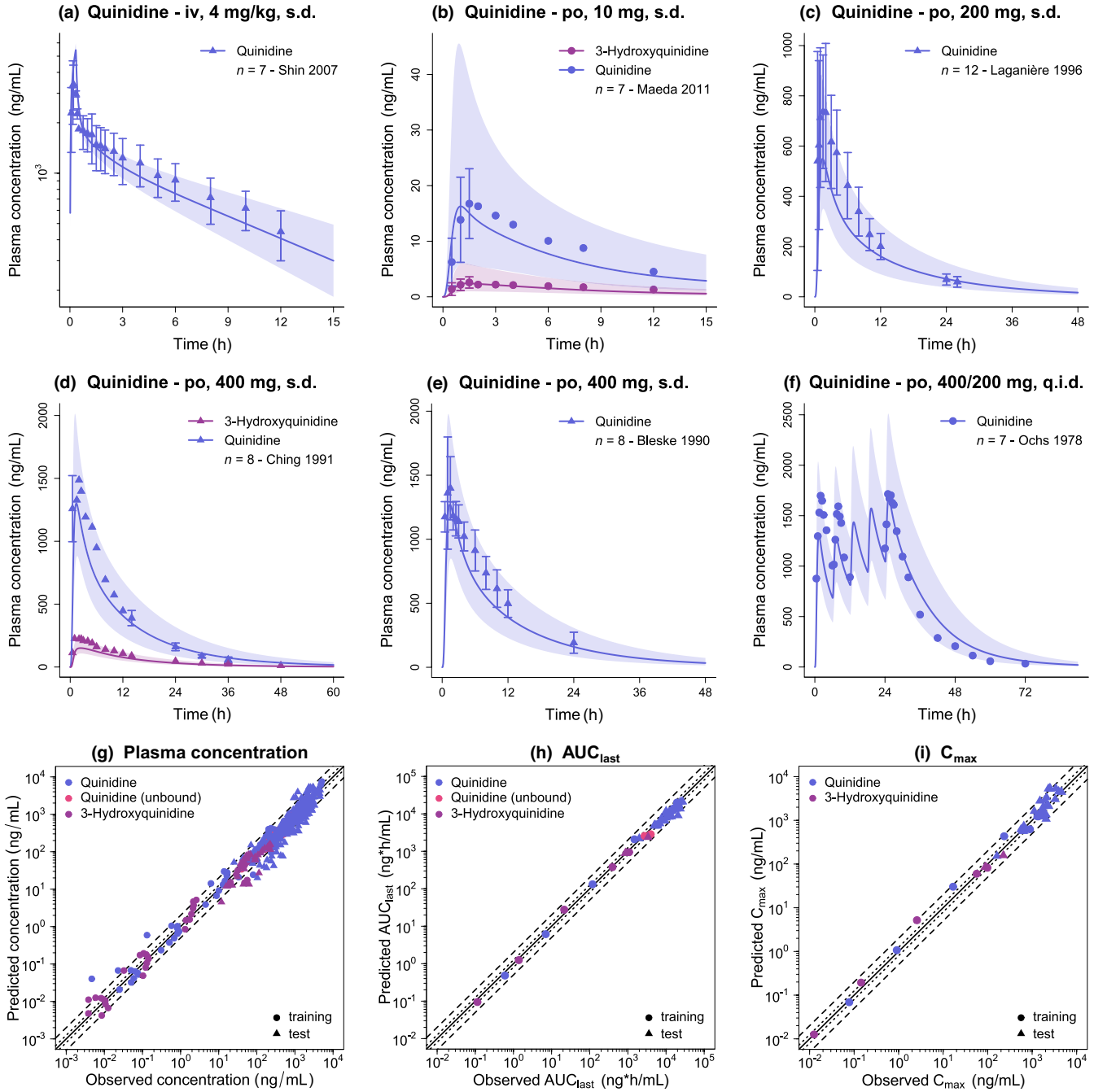

FIGURE 1 Quinidine physiologically-based pharmacokinetic modeling performance evaluation. (a–f) Predicted compared to observed plasma concentration-time profiles of quinidine and 3-hydroxyquinidine after (a) intravenous and (b–f) oral administration. Population geometric means are shown as lines, geometric standard deviations are shown as shaded areas, and observed data are shown as dots (training dataset) and triangles (test dataset) (±standard deviation, if reported).[8,25–29] (g–i) Goodness-of-fit plots comparing predicted and observed (g) plasma concentrations, (h) area under the plasma concentration-time curve calculated between first and last concentration measurement (AUC_{last}) and (i) maximum plasma concentration (C_{max}) values. The solid line represents the line of identity, whereas 1.25-fold and two-fold prediction limits are shown as dotted and dashed lines, respectively. Doses indicate (a) quinidine gluconate and (b–f) quinidine sulfate administration. Respective doses of quinidine base were calculated and incorporated in simulations. iv, intravenous; *n*, number of study participants; po, oral, q.i.d., four times daily; s.d., single dose.

training dataset, and three of three 3-hydroxyquinidine test dataset predicted plasma concentration profile MRDs were less than two. For quinidine, 10 of 10 (training dataset) and 32 of 33 (test dataset) AUC_{last} GMFEs, and eight of eight (training dataset) and 30 of 33 (test dataset) C_{max} GMFEs were below two. For 3-hydroxyquinidine, five of five (training dataset) and three of three (test dataset) AUC_{last} GMFEs, and four of five (training dataset) and

three of three (test dataset) C_{max} GMFEs values were within the two-fold threshold. For quinidine, all predicted V_d and half-life values are within twofold of observed values. The calculated MRD and GMFE values for all studies are listed and summarized in Tables S6–S9.

A local sensitivity analysis using a multiple dose simulation of 200 mg quinidine sulfate (protocol according to Ochs et al.[25]) revealed that the quinidine model is sensitive to the quinidine fraction unbound in plasma and lipophilicity (both implemented as fixed literature values). The 3-hydroxyquinidine model is sensitive to 3-hydroxyquinidine fraction unbound, the Michaelis–Menten (both fixed values from the literature) and catalytic-rate constants (optimized) describing the CYP3A4-dependent metabolism of quinidine to 3-hydroxyquinidine and the optimized unspecific hepatic clearance process. Parameters evaluated during sensitivity analysis are provided in Table S10, results of the local sensitivity analyses are visualized in Figures S17 and S18.

DD(G)I modeling network

The quinidine model was evaluated within a comprehensive CYP2D6-CYP3A4-P-gp DD(G)I network (Figure 2). Information about published perpetrator and victim models' relevant interaction constants and model parameters are provided in Tables S11 and S12. A total of nine quinidine and four 3-hydroxyquinidine profiles obtained from eight DDI studies were utilized to assess the quinidine-3-hydroxyquinidine model performance in DDI scenarios affected by CYP3A4 and P-gp perpetrator drugs. Here, one study described the carbamazepine-quinidine DDI, two studies the cimetidine-quinidine DDI, and one study each the fluvoxamine-quinidine, itraconazole-quinidine, and omeprazole-quinidine DDIs, one study the rifampicin-quinidine DDI, and one study the verapamil-quinidine DDI. Interaction parameters for the various modes of interaction (see Figure 2) were gathered from literature reports, if not already defined in the respective model files. To inform the relative contributions of CYP3A4 and P-gp to quinidine metabolism and transport during quinidine model building, data from the carbamazepine-quinidine DDI (i.e., the extent of 3-hydroxyquinidine formed) was included in the training dataset. Data from the remaining DDIs were used for the evaluation of model predictive performance.

Moreover, eight studies were utilized to model DD(G)I scenarios where quinidine and 3-hydroxyquinidine act as inhibitors of CYP2D6 and P-gp. One study was available to assess the effect of CYP2D6 inhibition via quinidine and 3-hydroxyquinidine for the quinidine-metoprolol interaction and one study on the effect of the quinidine-paroxetine-dextromethorphan interactions. Additionally, several DDGI studies in subpopulations with different CYP2D6 activities were available for the victim drugs dextromethorphan (two studies), metoprolol (one study), and mexiletine (one study). Finally, two studies reported data on the quinidine-digoxin DDI (P-gp inhibition). Multiple studies included plasma concentration-time profiles of multiple compounds, including parent victim drugs, respective enantiomers, and metabolites. For competitive inhibition of CYP2D6, K_i values of 0.017 μmol/L (quinidine[30]) and 2.30 μmol/L (3-hydroxyquinidine[10]) were incorporated from the literature as well as a K_i value of 0.10 μmol/L to describe competitive inhibition of P-gp by quinidine.[31] Information about all utilized studies covering perpetrator and victim drug regimens and subject demographics are provided in Tables S13 and S14.

Population predictions of victim plasma concentration-time profiles alone or with perpetrator co-administration compared to observed data demonstrated a good DD(G)I model performance (Figures 3 and 4). Semilogarithmic and linear plots of all studies are shown in Figures S19–S28.

Graphical comparisons of predicted and observed DD(G)I AUC_{last} and C_{max} ratios of all investigated DD(G)Is are shown in Figures 5, S29, and S30, revealing adequate model performance of quinidine either as a victim or perpetrator drug. For quinidine as CYP3A4 and P-gp victim, 12 of 13 and 12 of 13 of DDI AUC_{last} and C_{max} ratios were within two-fold of observed values and 12 of 13 and 11 of 13 within the prediction success limits proposed by Guest et al.[24] with mean GMFEs of 1.29 and 1.34, respectively. Overall, DD(G)Is with quinidine as a perpetrator of CYP2D6 and P-gp and the victim drugs dextromethorphan, digoxin, metoprolol, mexiletine, and paroxetine were accurately predicted with 15 of 17 DD(G)I AUC_{last} ratios and 13 of 15 DD(G)I C_{max} ratios within two-fold of the corresponding observed ratios. All AUC_{last} and C_{max} ratios grouped by the respective victim drugs and their metabolites are listed in Tables S15 and S16.

DISCUSSION

In this study, we present a newly developed whole-body parent-metabolite PBPK model of quinidine and its major metabolite 3-hydroxyquinidine. The good predictive performance simulating quinidine and 3-hydroxyquinidine plasma concentration-time profiles was evaluated by established graphical and quantitative measures. The model was further evaluated by simulating various modes of interactions in a comprehensive DD(G)I network. Here, the final model could be successfully linked with a diverse set of previously published CYP3A4 and P-gp perpetrator

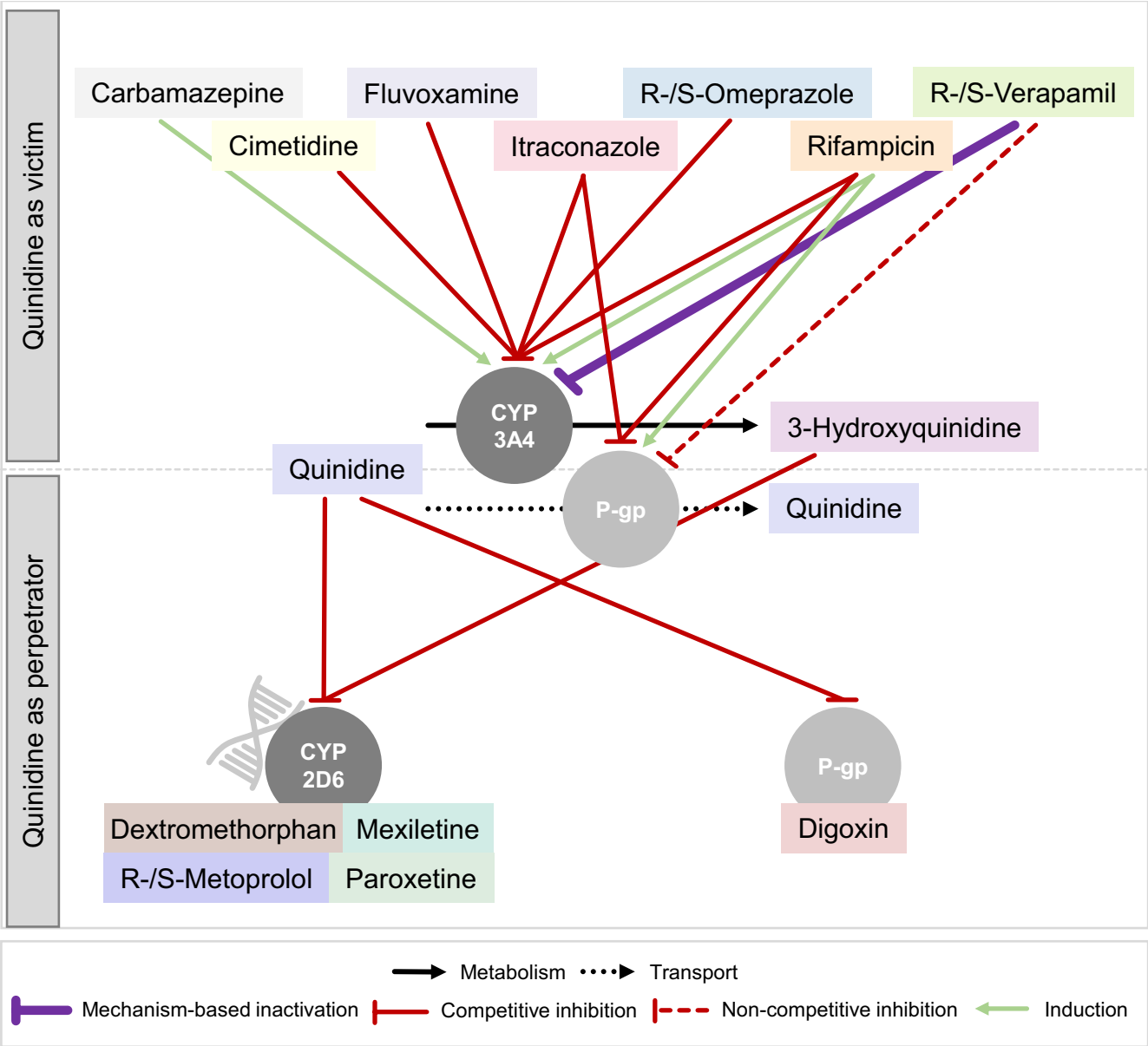

FIGURE 2 Quinidine drug–drug(–gene) interaction (DD(G)I) modeling network. (Upper panel) With quinidine acting as cytochrome P450 (CYP) 3A4 and P-glycoprotein (P-gp) victim drug, interactions with carbamazepine, cimetidine, fluvoxamine, itraconazole, R-/S-omeprazole, rifampicin, and R-/S-verapamil were modeled, taking different modes of interaction into account. (Lower panel) With quinidine acting as CYP2D6 and P-gp perpetrator drug, interactions were modeled with dextromethorphan, mexiletine, R-/S-metoprolol, and paroxetine in subjects with varying CYP2D6 activity (depending on data availability) and with digoxin (P-gp substrate).

models (quinidine acting as victim) as well as CYP2D6 and P-gp victim models (quinidine acting as perpetrator) to predict various DD(G)I scenarios.

Quinidine ADME processes include efflux via P-gp[5] (e.g., located at the intestinal barrier and, therefore, affecting oral bioavailability). Furthermore, quinidine is described as a substrate of CYP3A4 in vitro[7] and this enzyme can be attributed to the extensive first-pass metabolism of quinidine.[6] The reported quinidine average oral bioavailability of 70%[6] is in good agreement with our model simulations of oral bioavailabilities ranging from 37% (0.1 mg single dose) to 79% (600 mg single dose) and is in line with the proposed P-gp saturation as one cause for its nonlinear pharmacokinetics.[8] Total fractions of dose metabolized via CYP3A4 vary between very low (17%) and high doses (65%) of quinidine. This might be a result of varying fraction absorbed due to P-gp activity at the intestinal barrier and therefore a different impact of first-pass metabolism in the intestinal mucosa and in the liver. Another site of the body where P-gp contributes to quinidine pharmacokinetics is in tubule cells, where P-gp is responsible for the active tubular secretion of quinidine.

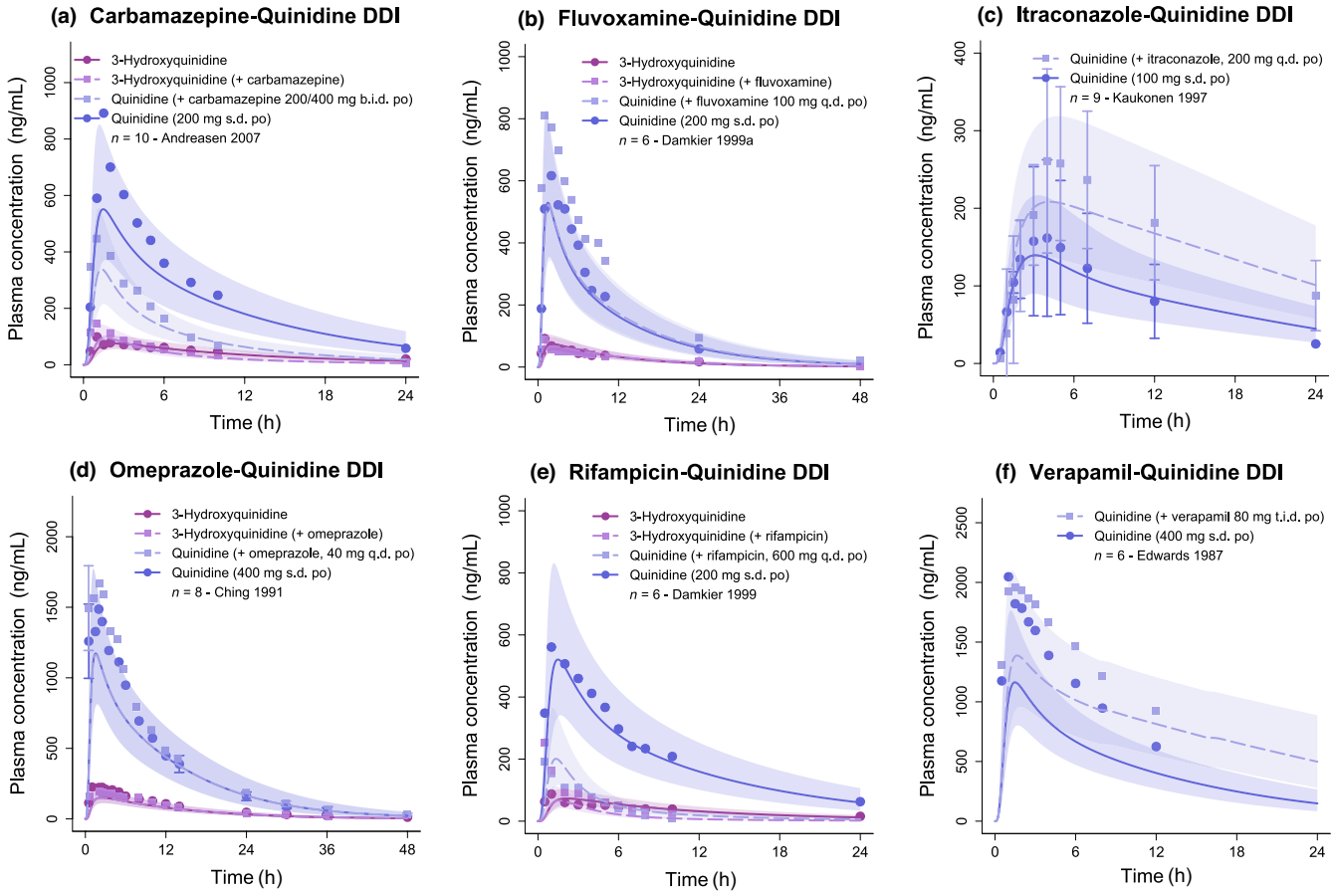

FIGURE 3 Modeled drug–drug interactions (DDIs) involving quinidine as cytochrome P450 (CYP) 3A4 and P-glycoprotein (P-gp) victim. (a–f) Predicted compared to observed plasma concentration-time profiles of quinidine and 3-hydroxyquinidine alone and after pretreatment with and/or concomitant administration of (a) carbamazepine, (b) fluvoxamine, (c) itraconazole, (d) R-/S-omeprazole, (e) rifampicin, and (f) R-/S-verapamil (low verapamil dose regimen). Population geometric means are shown as lines (solid: quinidine and 3-hydroxyquinidinde alone, dashed: quinidine and 3-hydroxyquinidinde during DDI), geometric standard deviations are shown as shaded areas and observed data are shown as dots (control) and squares (DDI) (±standard deviation, if reported).[26,32–36] Quinidine doses indicate quinidine sulfate administration. Respective doses of quinidine base were calculated and incorporated in simulations. b.i.d., twice daily; *n*, number of study participants; po, oral; q.d., once daily; s.d., single dose; t.i.d, three times daily.

Profiles of the amount of quinidine excreted in urine over time have been included in parameter optimizations to inform this process. However, urinary excretion of quinidine has been described to be pH dependent,[32] which might explain challenging the description and prediction of urine data.

Metabolism via CYP3A4 shows the largest contribution in vitro compared to other CYP enzymes.[7] However, in vivo metabolism via CYP3A4 was not easily assessable from literature reports, because competitive inhibitors of CYP3A4 in clinical DDI studies showed only a small effect on quinidine plasma concentrations.[26,33] Therefore, plasma concentration-time profiles of quinidine and 3-hydroxyquinidine during interaction with carbamazepine, a CYP3A4 inducer, were consulted to serve as a surrogate for lacking in vitro and in vivo data to estimate the relative contribution of CYP3A4 to quinidine metabolism. This approach has been successfully applied before, to estimate the previously unknown contribution of CYP3A4 and tubular secretion (also mediated via P-gp) in a PBPK model of trimethoprim.[17] Here, a DDI study with rifampicin, a CYP3A4 and P-gp competitive inhibitor and inducer, was included in the training dataset during the model building process, leading to a favorable description of trimethoprim concentrations in plasma and fractions excreted in urine.[17]

The co-administration of quinidine and various perpetrator and victim drugs covering different modes of interaction on several targets has been investigated in this work. To cover relevant interaction mechanisms and targets, the main metabolite of quinidine, 3-hydroxyquinidine, was included, (i) to adequately assess the impact of CYP3A4 perpetrator drugs and (ii) to incorporate its interaction potential, as inhibition of CYP2D6 has also been reported for the metabolite.[10]

Cimetidine is classified as a weak clinical inhibitor of CYP3A4 by the FDA.[5] In the model, inhibition of CYP3A4

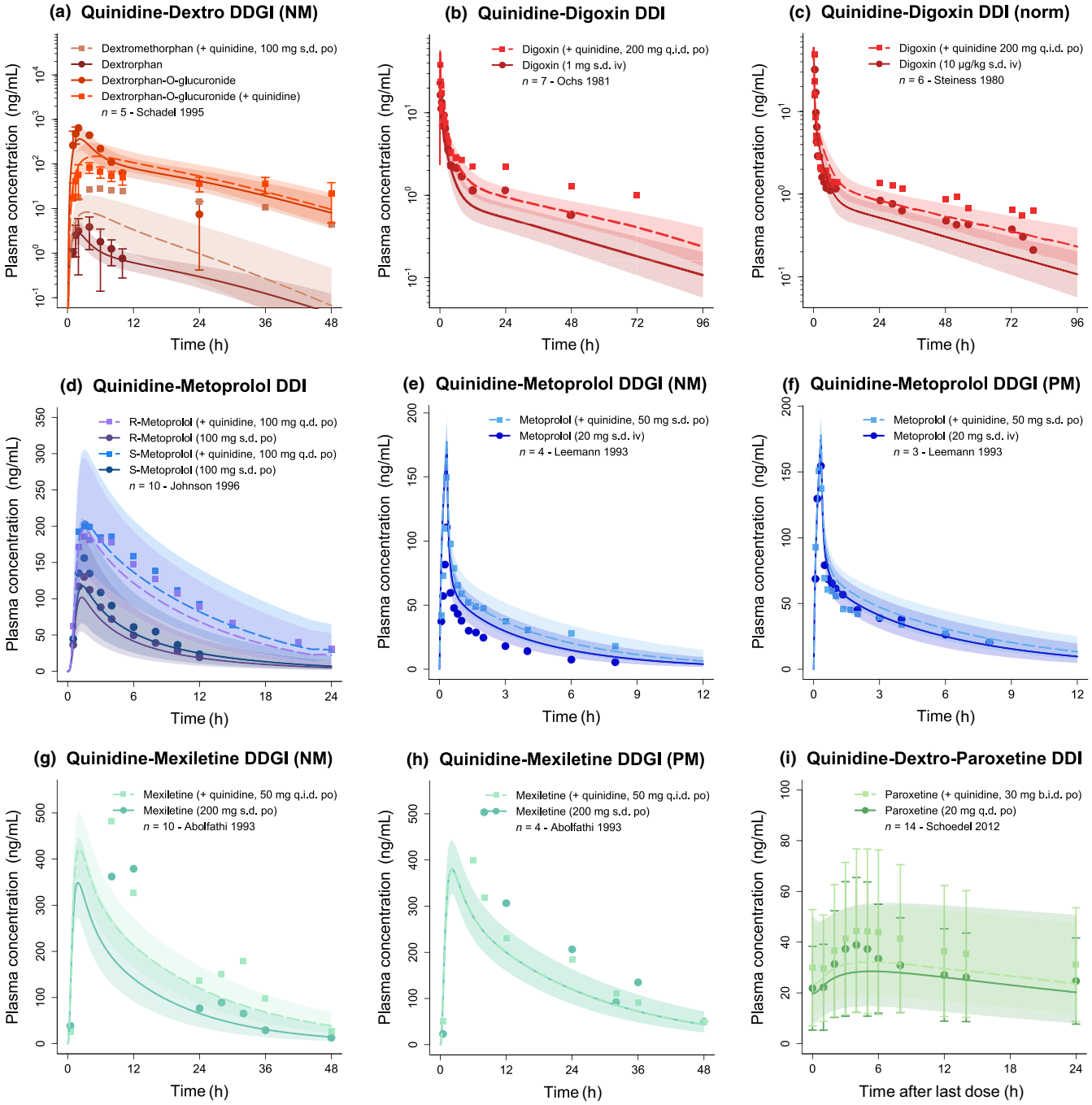

FIGURE 4 Modeled drug–drug(–gene) interactions (DD(G)Is) involving quinidine as cytochrome P450 (CYP) 2D6 and P-glycoprotein (P-gp) perpetrator. (a–i) Predicted compared to observed plasma concentration-time profiles of (a) dextromethorphan (+ metabolites) in CYP2D6 normal metabolizers (NMs), (b, c) digoxin, (d) R-/S-metoprolol, (e, f) racemic metoprolol (low quinidine dose regimen), (g, h) mexiletine, and (i) paroxetine (in combination with dextromethorphan) alone and after pretreatment with and/or concomitant administration of quinidine. Population geometric means are shown as lines (solid: victim alone, dashed: victim during drug-drug interaction [DDI]), geometric standard deviations are shown as shaded areas and observed data are shown as dots (control) and squares (DDI) (± standard deviation, if reported).[11,37–42] Quinidine doses indicate quinidine sulfate administration. Respective doses of quinidine base were calculated and incorporated in simulations. b.i.d., twice daily; iv, intravenous; *n*, number of study participants; norm, dose-normalized; PM, CYP2D6 poor metabolizer; po, oral; q.d., once daily; q.i.d., four times daily; s.d., single dose.

by cimetidine is incorporated, and the model has been evaluated in DDI predictions with the CYP3A4 index substrate midazolam.[5,12] Linking the cimetidine model to the newly developed quinidine model, no interaction effect could be observed via simulation. However, as a small interaction effect could be observed in clinical studies,[43,44]

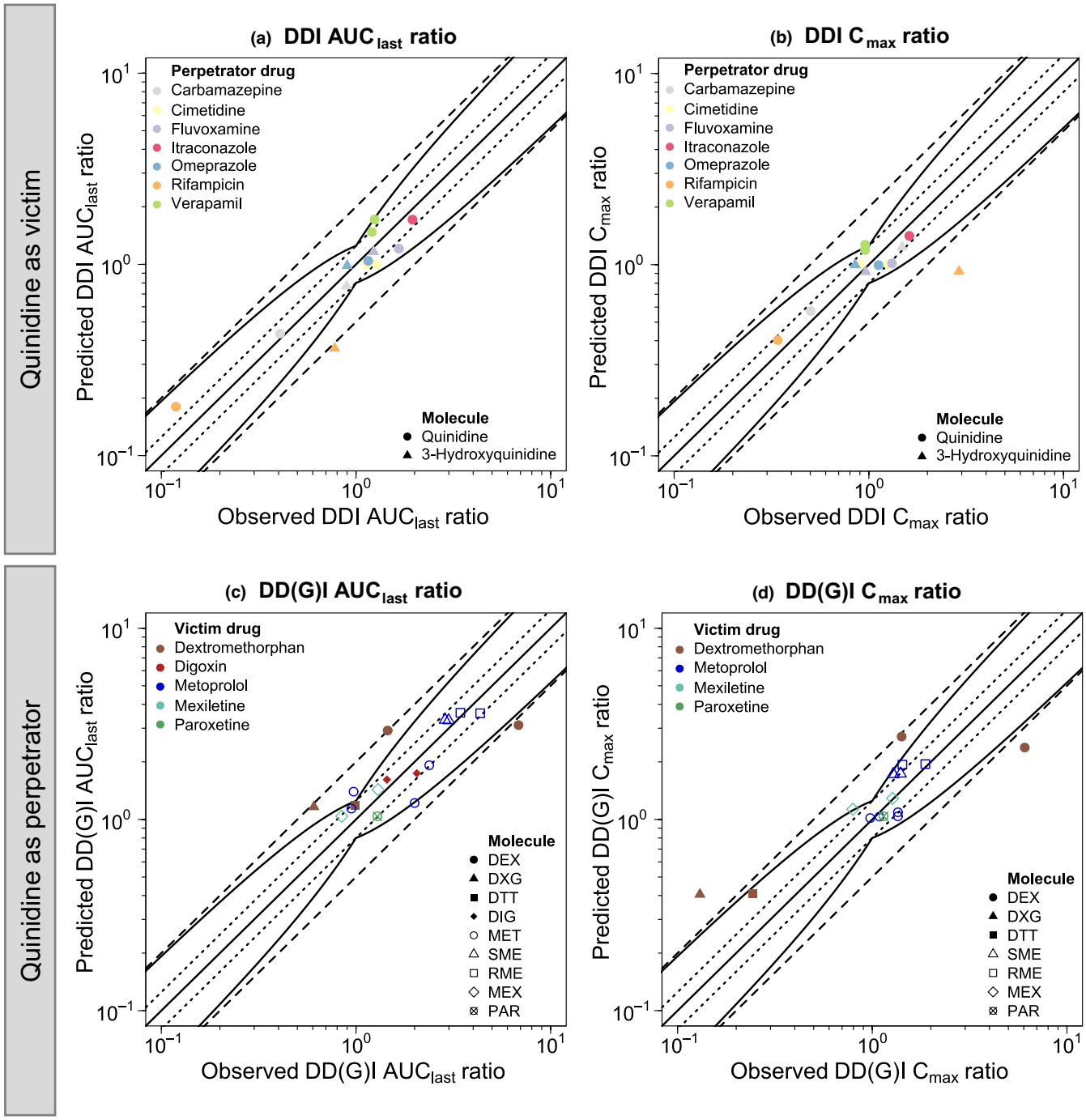

FIGURE 5 Quinidine drug–drug(–gene) interaction (DD(G)I) model performance evaluation. (a, b) For quinidine acting as a cytochrome P450 (CYP) 3A4 and P-glycoprotein (P-gp) victim, predicted drug–drug interaction (DDI) (a) area under the plasma concentration-time curve calculated between the first and last concentration measurement (AUC_{last}) and (b) maximum plasma concentration (C_{max}) ratios of quinidine and 3-hydroxyquinidine are plotted against their respective observed values after pretreatment with and/or concomitant administration of carbamazepine, cimetidine, fluvoxamine, itraconazole, R-/S-omeprazole, rifampicin, and R-/S-verapamil.[26,32–36,43,44] (c, d) For quinidine acting as a CYP2D6 and P-gp perpetrator, predicted DD(G)I (c) AUC_{last} and (d) C_{max} ratios of dextromethorphan (DEX), dextrorphan-O-glucuronide (DXG), total dextrorphan (DTT), digoxin (DIG), metoprolol (MET), S-metoprolol (SME), and R-metoprolol (RME), mexiletine (MEX) and paroxetine (PAR) are plotted against their respective observed values after pretreatment with and/or concomitant administration of quinidine.[11,37–42,45] The solid line represents the line of identity, whereas 1.25-fold and two-fold prediction limits are shown as dotted and dashed lines, respectively. Prediction success limits proposed by Guest et al.[24] are shown as curved lines (including 20% variability).

this effect might be attributed to interaction processes which could not be attributed to incorporated processes. For instance, cimetidine is a known inhibitor of several other proteins (e.g., transporters and other metabolic enzymes),[12] and further transport mechanisms have been discussed for quinidine but not incorporated due to limited information.

Quinidine has been described as P-gp substrate and inhibitior,[5] and mutual interactions with other drugs that can also be classified as P-gp substrate and inhibitor or inducer are plausible. This was considered for the modeled interaction between quinidine and verapamil by incorporating interaction parameters for both quinidine and verapamil. However, in the analyzed verapamil-quinidine interaction study by Edwards et al.,[34] only quinidine plasma concentrations were reported with no profiles of verapamil. Therefore, the effect of quinidine on verapamil pharmacokinetics could not be evaluated.

Regarding the rifampicin-quinidine DDI, which involves induction and inhibition of CYP3A4 (metabolism of quinidine and 3-hydroxyquinidine) and P-gp (transport of quinidine), plasma concentration-time profiles, DDI AUC_{last} and C_{max} ratios are well-predicted for the parent drug quinidine. However, for the metabolite, AUC_{last} and C_{max} are underpredicted during the DDI. This might be attributed to CYP3A4 involved in the formation as well as the metabolism of 3-hydroxyquinidine with an unknown extent of contribution for the latter process. In addition, other enzymes that might be involved in the metabolism could be the subject of induction by rifampicin. Additionally, P-gp may play a role in the active transport of 3-hydroxyquinidine. This could account for the underestimation of 3-hydroxyquinidine levels in urine, although this process was not included in the model due to insufficient data. Conducting in vitro studies to determine the extent of inducible CYP enzymes involved in 3-hydroxyquinidine metabolism, as well as the potential contribution of P-gp, may enhance our understanding of DDI mechanisms. This information could then be incorporated into the model as it becomes available.

The investigated DDIs with CYP2D6 victim drugs could be satisfactorily predicted with the model. For the modeled DDGIs with dextromethorphan (two studies)[37,45] and metoprolol (one study)[11] as victim drugs, CYP2D6-dependent metabolism was estimated from the control studies without an interaction partner to cover the extensive unexplained interindividual variability in CYP2D6 activity (Table S14). Subsequently, these adjustments were carried over to the DDI simulations. These studies solely provided CYP2D6 phenotypes, however, applying a finer-scaled activity score-based system to classify polymorphic CYP2D6 activity has been shown to lead to accurate DGI modeling results.[13,14,23] Here, no quinidine DDGI studies reporting CYP2D6 genotypes or activity scores could be obtained from published literature. Hence, the quinidine DDGI model performance of such scenarios remained unassessed, but the model could be extended in the future as far as such studies come available. For mexiletine, plasma-concentration-time profiles are slightly underpredicted, especially in CYP2D6 normal metabolizers. However, the profiles reported in the study by Abolfathi et al.[38] show representative profiles rather than mean profiles. Additionally, the variability in CYP2D6 activity and also other metabolic processes, such as CYP1A2-mediated metabolism, might contribute to interindividual variability of mexiletine pharmacokinetics. Of note, the model has a tendency to underpredict mexiletine clearance in normal metabolizers, as mentioned by the authors of the model publication,[21] likely resulting in a slight misprediction of mexiletine in both control and DDI scenarios. Nonetheless, DDI AUC_{last} and C_{max} ratios were within the prediction success limits proposed by Guest et al.,[24] indicating good performance of the quinidine model in CYP2D6 DDI scenarios.

Several PBPK model analyses have been published for quinidine. These focused on DDI predictions with quinidine as either a perpetrator drug with, for example, tramadol,[46] nifedipine and metoprolol[47] or as a victim drug, in DDI scenarios with rifampicin[48] or itraconazole and verapamil.[49] Furthermore, one article presented a PBPK/pharmacodynamic model of quinidine to investigate its effect on the length of QT-interval.[50] In contrast to previous work, our whole-body PBPK model covers the formation of the main quinidine metabolite, 3-hydroxyquinidine (mainly via CYP3A4) for correct interaction predictions considering CYP3A4 and CYP2D6 as well as the mechanistic implementation of ADME processes for both compounds (e.g., quinidine transport via P-gp). Furthermore, several DD(G)I scenarios could be successfully described and predicted within a comprehensive interaction network, evaluating quinidine as a perpetrator (CYP2D6 and P-gp) and as a victim drug (CYP3A4 and P-gp). Moreover, the presented quinidine PBPK model was developed using a variety of quinidine and 3-hydroxyquinidine concentration-time profiles covering two routes of administration (intravenous and oral administration), a large dosing range (0.1–600 mg) and both single and multiple administrations. The presented quinidine model focuses on quinidine sulfate formulations for oral administration, but implementation of further formulations (e.g., extended-release), could be performed with the model once required data (e.g., in vitro dissolution profiles), become available.

To conclude, this work presents a comprehensive quinidine whole-body PBPK model that describes and predicts quinidine and 3-hydroxyquinidine

pharmacokinetics administered alone or in combination with CYP3A4 and P-gp inhibitors or inducers. Moreover, the model has demonstrated its predictive performance in interaction scenarios with a diverse set of CYP2D6 and P-gp victim drugs—also in subjects with altered CYP2D6 activity due to genetic polymorphisms. The presented network can be extended in the future by integrating more interaction studies on further perpetrator and victim drugs. The PBPK model files are provided to the modeling community (http://models.clinicalpharmacy.me/) to assist model-informed drug development through further investigations on DD(G)Is involving quinidine.

AUTHOR CONTRIBUTIONS

All authors wrote the manuscript. D.F., S.R., D.S., and T.L. designed the research. D.F. and S.R. performed the research. D.F., S.R., F.Z.M., and D.S. analyzed the data.

FUNDING INFORMATION

This work is part of the Horizon 2020 INSPIRATION (Qualified Open Systems Pharmacology Modeling Network of Drug–Drug–Gene-Interactions) project. The INSPIRATION project (FKZ 031L0241) is supported by the German Federal Ministry of Education and Research under the framework of ERACoSysMed. M.S. was supported in parts by the Robert Bosch Stiftung Stuttgart, Germany, and the Deutsche Forschungsgemeinschaft (DFG) under Germany's Excellence Strategy-EXC 2180-390900677.

CONFLICT OF INTEREST STATEMENT

D.T. is an employee of Sanofi. D.T. uses Open Systems Pharmacology software, tools, or models in his professional role. D.T. and T.L. are members of the Open Systems Pharmacology Management Team. S.F. uses Open Systems Pharmacology software, tools, or models in his professional role. S.F. is a member of the Open Systems Pharmacology Sounding Board. All other authors declared no competing interest for this work.

ORCID

Simeon Rüdesheim https://orcid.org/0000-0002-5741-2511
Matthias Schwab https://orcid.org/0000-0002-9984-075X
Thorsten Lehr https://orcid.org/0000-0002-8372-1465

REFERENCES

1. Ingelman-Sundberg M. Genetic polymorphisms of cytochrome P450 2D6 (CYP2D6): clinical consequences, evolutionary aspects and functional diversity. *Pharmacogenomics J*. 2005;5:6-13.
2. Türk D, Fuhr LM, Marok FZ, et al. Novel models for the prediction of drug-gene interactions. *Expert Opin Drug Metab Toxicol*. 2021;17:1293-1310.
3. Storelli F, Matthey A, Lenglet S, Thomas A, Desmeules J, Daali Y. Impact of CYP2D6 functional allelic variations on phenoconversion and drug–drug interactions. *Clin Pharmacol Ther*. 2018;104:148-157.
4. Vitali Serdoz L, Rittger H, Furlanello F, Bastian D. Quinidine–a legacy within the modern era of antiarrhythmic therapy. *Pharmacol Res*. 2019;144:257-263.
5. U.S. Food and Drug Administration. Drug development and drug interactions: table of substrates, inhibitors and inducers. 2022 https://www.fda.gov/drugs/drug-interactions-labeling/drug-development-and-drug-interactions-table-substrates-inhibitors-and-inducers
6. Guentert TW, Holford NHG, Coafes PE, Upton RA, Riegelman S. Quinidine pharmacokinetics in man: choice of a disposition model and absolute bioavailability studies. *J Pharmacokinet Biopharm*. 1979;7:315-330.
7. Nielsen TL, Rasmussen BB, Flinois JP, Beaune P, Brosen K. In vitro metabolism of quinidine: the (3S)-3-hydroxylation of quinidine is a specific marker reaction for cytochrome P-4503A4 activity in human liver microsomes. *J Pharmacol Exp Ther*. 1999;289:31-37.
8. Maeda K, Takano J, Ikeda Y, et al. Nonlinear pharmacokinetics of Oral quinidine and verapamil in healthy subjects: a clinical microdosing study. *Clin Pharmacol Ther*. 2011;90:263-270.
9. McLaughlin LA, Paine MJI, Kemp CA, et al. Why is quinidine an inhibitor of cytochrome P450 2D6? The role of key active-site residues in quinidine binding. *J Biol Chem*. 2005;280:38617-38624.
10. Ching MS, Blake CL, Ghabrial H, et al. Potent inhibition of yeast-expressed CYP2D6 by dihydroquinidine, quinidine, and its metabolites. *Biochem Pharmacol*. 1995;50:833-837.
11. Leemann TD, Devi KP, Dayer P. Similar effect of oxidation deficiency (debrisoquine polymorphism) and quinidine on the apparent volume of distribution of (+/−)-metoprolol. *Eur J Clin Pharmacol*. 1993;45:65-71.
12. Hanke N, Türk D, Selzer D, et al. A comprehensive whole-body physiologically based pharmacokinetic drug-drug-gene interaction model of metformin and cimetidine in healthy adults and Renally impaired individuals. *Clin Pharmacokinet*. 2020;59:1419-1431.
13. Rüdesheim S, Wojtyniak JG, Selzer D, et al. Physiologically based pharmacokinetic modeling of metoprolol enantiomers and α-hydroxymetoprolol to describe CYP2D6 drug-gene interactions. *Pharmaceutics*. 2020;12:1200.
14. Rüdesheim S, Selzer D, Fuhr U, Schwab M, Lehr T. Physiologically-based pharmacokinetic modeling of dextromethorphan to investigate interindividual variability within CYP2D6 activity score groups. *CPT Pharmacometrics Syst Pharmacol*. 2022;11:494-511.
15. Wendl T, Frechen S, Gerisch M, Heinig R, Eissing T. Physiologically-based pharmacokinetic modeling to predict CYP3A4-mediated drug-drug interactions of finerenone. *CPT Pharmacometrics Syst Pharmacol*. 2022;11:199-211.
16. Woodruff TJ, Bois FY. Optimization issues in physiological toxicokinetic modeling: a case study with benzene. *Toxicol Lett*. 1993;69:181-196.

17. Türk D, Hanke N, Lehr T. A physiologically-based pharmacokinetic model of trimethoprim for MATE1, OCT1, OCT2, and CYP2C8 drug-drug-gene interaction predictions. *Pharmaceutics*. 2020;12:1074.
18. Fuhr LM, Marok FZ, Hanke N, Selzer D, Lehr T. Pharmacokinetics of the CYP3A4 and CYP2B6 inducer carbamazepine and its drug–drug interaction potential: a physiologically based pharmacokinetic modeling approach. *Pharmaceutics*. 2021;13:270.
19. Britz H, Hanke N, Volz AK, et al. Physiologically-based pharmacokinetic models for CYP1A2 drug-drug interaction prediction: a modeling network of fluvoxamine, theophylline, caffeine, rifampicin, and midazolam. *CPT Pharmacometrics Syst Pharmacol*. 2019;8:296-307.
20. Hanke N, Frechen S, Moj D, et al. PBPK models for CYP3A4 and P-gp DDI prediction: a modeling network of rifampicin, itraconazole, clarithromycin, midazolam, alfentanil, and digoxin. *CPT Pharmacometrics Syst Pharmacol*. 2018;7:647-659.
21. Kanacher T, Lindauer A, Mezzalana E, et al. A physiologically-based pharmacokinetic (PBPK) model network for the prediction of CYP1A2 and CYP2C19 drug-drug-gene interactions with fluvoxamine, omeprazole, S-mephenytoin, moclobemide, tizanidine, mexiletine, ethinylestradiol, and caffeine. *Pharmaceutics*. 2020;12:1-15.
22. Hanke N, Türk D, Selzer D, et al. A mechanistic, enantioselective, physiologically based pharmacokinetic model of verapamil and Norverapamil, built and evaluated for drug–drug interaction studies. *Pharmaceutics*. 2020;12:556.
23. Rüdesheim S, Selzer D, Mürdter T, et al. Physiologically based pharmacokinetic modeling to describe the CYP2D6 activity score-dependent metabolism of paroxetine, atomoxetine and risperidone. *Pharmaceutics*. 2022;14:1734.
24. Guest EJ, Aarons L, Houston JB, Rostami-Hodjegan A, Galetin A. Critique of the two-fold measure of prediction success for ratios: application for the assessment of drug-drug interactions. *Drug Metab Dispos*. 2011;39:170-173.
25. Ochs HR, Greenblatt DJ, Woo E, Franke K, Pfeifer HJ, Smith TW. Single and multiple dose pharmacokinetics of oral quinidine sulfate and gluconate. *Am J Cardiol*. 1978;41:770-777.
26. Ching MS, Elliott SL, Stead CK, et al. Quinidine single dose pharmacokinetics and pharmacodynamics are unaltered by omeprazole. *Aliment Pharmacol Ther*. 1991;5:523-531.
27. Shin J-G, Kang WK, Shon JH, et al. Possible interethnic differences in quinidine-induced QT prolongation between healthy Caucasian and Korean subjects. *Br J Clin Pharmacol*. 2007;63:206-215.
28. Laganière S, Davies RF, Carignan G, et al. Pharmacokinetic and pharmacodynamic interactions between diltiazem and quinidine. *Clin Pharmacol Ther*. 1996;60:255-264.
29. Bleske BE, Carver PL, Annesley TM, Bleske JRM, Morady F. The effect of ciprofloxacin on the pharmacokinetic and ECG parameters of quinidine. *J Clin Pharmacol*. 1990;30:911-915.
30. Moghadamnia AA, Rostami-Hodjegan A, Abdul-Manap R, Wright CE, Morice AH, Tucker GT. Physiologically based modelling of inhibition of metabolism and assessment of the relative potency of drug and metabolite: dextromethorphan vs. dextrorphan using quinidine inhibition. *Br J Clin Pharmacol*. 2003;56:57-67.
31. Lumen AA, Acharya P, Polli JW, Ayrton A, Ellens H, Bentz J. If the KI is defined by the free energy of binding to P-glycoprotein, which kinetic parameters define the IC50 for the Madin-Darby canine kidney II cell line overexpressing human multidrug resistance 1 confluent cell monolayer? *Drug Metab Dispos*. 2010;38:260-269.
32. Kaukonen KM, Olkkola KT, Neuvonen PJ. Itraconazole increases plasma concentrations of quinidine. *Clin Pharmacol Ther*. 1997;62:510-517.
33. Damkier P, Hansen LL, Brøsen K. Effect of fluvoxamine on the pharmacokinetics of quinidine. *Eur J Clin Pharmacol*. 1999;55:451-456.
34. Edwards DJ, Lavoie R, Beckman H, Blevins R, Rubenfire M. The effect of coadministration of verapamil on the pharmacokinetics and metabolism of quinidine. *Clin Pharmacol Ther*. 1987;41:68-73.
35. Andreasen A-H, Brøsen K, Damkier P. A comparative pharmacokinetic study in healthy volunteers of the effect of carbamazepine and oxcarbazepine on cyp3a4. *Epilepsia*. 2007;48:490-496.
36. Damkier P, Hansen LL, Brøsen K. Rifampicin treatment greatly increases the apparent oral clearance of quinidine. *Pharmacol Toxicol*. 1999;85:257-262.
37. Schoedel KA, Pope LE, Sellers EM. Randomized open-label drug-drug interaction trial of dextromethorphan/quinidine and paroxetine in healthy volunteers. *Clin Drug Investig*. 2012;32:157-169.
38. Abolfathi Z, Fiset C, Gilbert M, Moerike K, Bélanger PM, Turgeon J. Role of polymorphic debrisoquin 4-hydroxylase activity in the stereoselective disposition of mexiletine in humans. *J Pharmacol Exp Ther*. 1993;266:1196-1201.
39. Schadel M, Wu D, Otton SV, Kalow W, Sellers EM. Pharmacokinetics of dextromethorphan and metabolites in humans: influence of the CYP2D6 phenotype and quinidine inhibition. *J Clin Psychopharmacol*. 1995;15:263-269.
40. Ochs HR, Bodem G, Greenblatt DJ. Impairment of digoxin clearance by coadministration of quinidine. *J Clin Pharmacol*. 1981;21:396-400.
41. Steiness E, Waldorff S, Hansen PB, Egebald H, Buch J, Egeblad H. Reduction of digoxin-induced inotropism during quinidine administration. *Clin Pharmacol Ther*. 1980;27:791-795.
42. Johnson JA, Burlew BS. Metoprolol metabolism via cytochrome P4502D6 in ethnic populations. *Drug Metab Dispos*. 1996;24:350-355.
43. Kolb KW, Garnett WR, Small RE, Vetrovec GW, Kline BJ, Fox T. Effect of cimetidine on quinidine clearance. *Ther Drug Monit*. 1984;6:306-312.
44. Hardy BG, Schentag JJ. Lack of effect of cimetidine on the metabolism of quinidine: effect on renal clearance. *Int J Clin Pharmacol Ther Toxicol*. 1983;26:388-391.
45. Capon DA, Bochner F, Kerry N, Mikus G, Danz C, Somogyi AA. The influence of CYP2D6 polymorphism and quinidine on the disposition and antitussive effect of dextromethorphan in humans. *Clin Pharmacol Ther*. 1996;60:295-307.
46. Long T, Cristofoletti R, Cicali B, et al. Physiologically based pharmacokinetic modeling to assess the impact of CYP2D6-mediated drug-drug interactions on tramadol and O-desmethyltramadol exposures via allosteric and competitive inhibition. *J Clin Pharmacol*. 2022;62:76-86.
47. Marsousi N, Desmeules JA, Rudaz S, Daali Y. Prediction of drug-drug interactions using physiologically-based pharmacokinetic models of CYP450 modulators included in Simcyp software. *Biopharm Drug Dispos*. 2018;39:3-17.

48. Asaumi R, Nunoya K, Yamaura Y, Taskar KS, Sugiyama Y. Robust physiologically based pharmacokinetic model of rifampicin for predicting drug–drug interactions via P-glycoprotein induction and inhibition in the intestine, liver, and kidney. *CPT Pharmacometrics Syst Pharmacol*. 2022;11:919-933.
49. Yamazaki S, Evers R, De Zwart L. Physiologically-based pharmacokinetic modeling to evaluate in vitro-to-in vivo extrapolation for intestinal P-glycoprotein inhibition. *CPT Pharmacometrics Syst Pharmacol*. 2022;11:55-67.
50. Chetty M, Rose RH, Abduljalil K, et al. Applications of linking PBPK and PD models to predict the impact of genotypic variability, formulation differences, differences in target binding capacity and target site drug concentrations on drug responses and variability. *Front Pharmacol*. 2014;5:258.

SUPPORTING INFORMATION

Additional supporting information can be found online in the Supporting Information section at the end of this article.

How to cite this article: Feick D, Rüdesheim S, Marok FZ, et al. Physiologically-based pharmacokinetic modeling of quinidine to establish a CYP3A4, P-gp, and CYP2D6 drug–drug–gene interaction network. *CPT Pharmacometrics Syst Pharmacol*. 2023;12:1143-1156. doi:10.1002/psp4.12981